SF2A 2012
S. Boissier, P. de Laverny, N. Nardetto, R. Samadi, D. Valls-Gabaud and H. Wozniak (eds)

UV AND OPTICAL POLARIZATION MODELING OF THERMAL ACTIVE GALACTIC NUCLEI: IMPACT OF THE NARROW LINE REGION

F. Marin[1] and R. W. Goosmann[1]

Abstract. In this research note, we start exploring the influence of the narrow line region (NLR) on the optical/UV continuum polarization of active galactic nuclei (AGN). We have upgraded our previous 3-component model of a thermal Seyfert nucleus that was composed of an equatorial, optically thin electron disc, a circumnuclear dusty torus, and a pair of collimated, optically thin electron winds. We have added a dusty extension with low optical depth to the outflows to account for continuum scattering and absorption inside the NLR. A spectropolarimetric comparison between our AGN models with and without NLR reprocessing is carried out. It turns out that the NLR can alter and even suppress the observed polarization dichotomy between type-1 and type-2 AGN. For type-2 AGN, it also significantly decreases the expected percentage of polarization and alters its spectral shape. While the NLR makes it more difficult to reproduce the observed polarization in type-1 objects, it helps to explain spectropolarimetry observations of type-2 objects. Further studies including clumpy media need to be carried out to obtain more precise constraints on the polarization dichotomy and the reprocessing geometry of AGN.

Keywords: Galaxies: active, Galaxies: Seyfert, Polarization, Radiative transfer, Scattering

1 Introduction

The unified model of active galactic nuclei (AGN) postulates that the emission of the continuum source and of the broad line region (BLR) is highly anisotropic because it is confined by the funnel of an obscuring dusty torus Antonucci (1993). A type-1 AGN has a visible BLR and is seen at a line of sight towards the central source that passes through the torus funnel. For a type-2 AGN, the view of the BLR is blocked by the torus body. The radiation from the center of the AGN can directly escape only along the polar regions of the funnel where it photo-ionizes conically shaped outflows. It was found that these winds are roughly stretched along the small scale radio-structure that is present in both radio-loud and radio-quiet AGN (Wilson & Ulvestad 1983). Beyond their sublimation radius, dust grains can form and coexist with the ionized outflow forming the so-called narrow line region (NLR). Capetti et al. (1999) showed that the NLR generally has a complex morphology consisting of filaments and compact emission knots (e.g. in NGC 4151) or narrow arcs (e.g. in Mrk 573). Due to this non-trivial geometry, it may be a difficult task to obtain accurate constraints on the NLR. However, spectropolarimetric studies of luminous AGN and numerical polarization modeling can improve our understanding if the complex radiative transfer between the various reprocessing regions is taken into account.

Goosmann & Gaskell (2007) investigated the continuum polarization induced by individual reprocessing regions, namely by dusty tori, polar outflows of various compositions, and equatorial scattering regions. Using this work as a starting point, we then modeled the optical/UV polarization emerging from a complex reprocessing system composed of three scattering components (Marin & Goosmann 2011; Marin et al. 2012b). The goal of the exhaustive study presented in Marin et al. (2012b) was to put solid constraints on the conditions that reproduce the observed polarization dichotomy between type-1 and type-2 AGN[i]. So far, we have left out the

[1] Observatoire Astronomique de Strasbourg, Université de Strasbourg, CNRS, UMR 7550, 11 rue de l'Université, 67000 Strasbourg, France. Email: frederic.marin@astro.unistra.fr

[i]Polarization is described as "parallel" when the $\vec{E}$-vector is aligned with the projected torus axis. We denote the difference between parallel and perpendicular polarization by the sign of the polarization percentage, P: a negative value of P stands for parallel polarization, a positive P for perpendicular one. Many type-1 AGN show parallel polarization while the polarization of type-2 objects is perpendicular (Antonucci 1982, 1983).

Table 1. Parameters of the individual scattering regions in our 3- and 4-component models. Note that for the polar outflow, the torus and the NLR, the half-opening angle is measured with respect to the vertical, symmetry axis of the model, while for the flared-disk the half-opening angle is taken with respect to the equatorial plane.

flared disk	dusty torus	ionized outflows	NLR
$R_{\min} = 3.10^{-4}$ pc	$R_{\min} = 0.25$ pc	$R_{\min} = 1$ pc	$R_{\min} = 20$ pc
$R_{\max} = 5.10^{-4}$ pc	$R_{\max} = 100$ pc	$R_{\max} = 10$ pc	$R_{\max} = 70$ pc
half-opening angle = 10°	half-opening angle = 30°	half-opening angle = 30°	half-opening angle = 30°
equat. optical depth = 1	equat. optical depth = 750	vertical optical depth = 0.03	vertical optical depth = 0.24
electron scattering	Mie scattering	electron scattering	Mie scattering

NLR as it is expected to decrease the total amount of parallel polarization in type-1 AGN. For more details on this we refer the reader to Marin et al. (2012b). In this short paper, we start to investigate the effects on the continuum polarization that can emerge from adding to our previously model an NLR-like polar scattering region that is filled with optically thin dust.

2 Model setup

The continuum emitting region of our thermal AGN is modeled by an isotropic, point-like source of unpolarized radiation having a power-law intensity spectrum $F_* \propto \nu^{-\alpha}$ with $\alpha = 1$. The source is closely surrounded by an electron-filled scattering ring producing the parallel polarization observed in type-1 objects (Antonucci 1984). At a larger distance and sharing the same equatorial plane, an obscuring, optically thick dusty torus blocks the radiation progressing towards edge-on directions. We assume that the torus collimates winds that are ejected from the inner accretion flow before they turn into a polar, hourglass-shaped outflow. These winds are optically thin, ionized and dominated by electron scattering. A complete description of the 3-component model can be found in Section 5 of Marin et al. (2012b). The model approximates the unified scheme of AGN and is optimized for the production of parallel polarization at a type-1 line of sight.

To study the effect of the NLR, we presently include extended, optically thin, dusty outflows sustaining the same half-opening angle and direction as the ionized winds. However, the amount of dust associated with the NLR is difficult to constrain from the observations due to 1) a complex filamentary structure between ionized gas and dust and 2) reddening corrections in the data reduction that can be a potential source of errors as the gas to dust composition is not known (Cracco et al. 2011). Taking into account that the fraction of dust in the NLR clouds must be smaller than in the circumnuclear region and in order to allow a large fraction of the radiation to escape in a polar direction, we fix the NLR opacity to a value significantly below unity (Hoenig et al. 2012). Table 1 summarizes the parameters of the reprocessing regions in our models.

We apply the latest public version of *STOKES*, a Monte Carlo radiative transfer code including a treatment of the polarization. The code was initially presented in Goosmann & Gaskell (2007) and new elements have been added by Marin et al. (2012b). The code is freely available on the Internet[ii]. It handles absorption and multiple scattering in a complex environment of emitting sources and reprocessing regions. Spectropolarimetric and polarization imaging results can be computed at any polar and azimuthal viewing angle. For more details on *STOKES* and its possible applications, we refer the reader to Marin et al. (2012b) and references therein.

3 Spectropolarimetric results

The resulting polarization percentage P and the fraction, F/F_*, of the central flux, F_*, as a function of the viewing angle for both the 3-component and the 4-component model are shown in Fig.1. As expected, the overall polarization behavior for the model including the NLR (Fig.1, top left) is different from the results obtained for the 3-component model (Fig.1, top right). When adding the NLR, the global amount of polarization in type-2 objects decreases due to a combination of effects; the polarized flux from the ionized outflows is diluted by the relatively weaker polarization of the flux coming from the NLR. Note that for our dust mixture (Mathis et al. 1977) the theoretical polarization degree produced by a single Mie scattering event reaches a maximum value of 35% at 8000 Å, while for electron scattering P is as high as 100%. The dilution from polar Mie scattering in the NLR is particularly efficient at edge-on viewing angles and P decreases by a factor of ~ 3 in comparison to the

[ii] http://www.stokes-program.info/

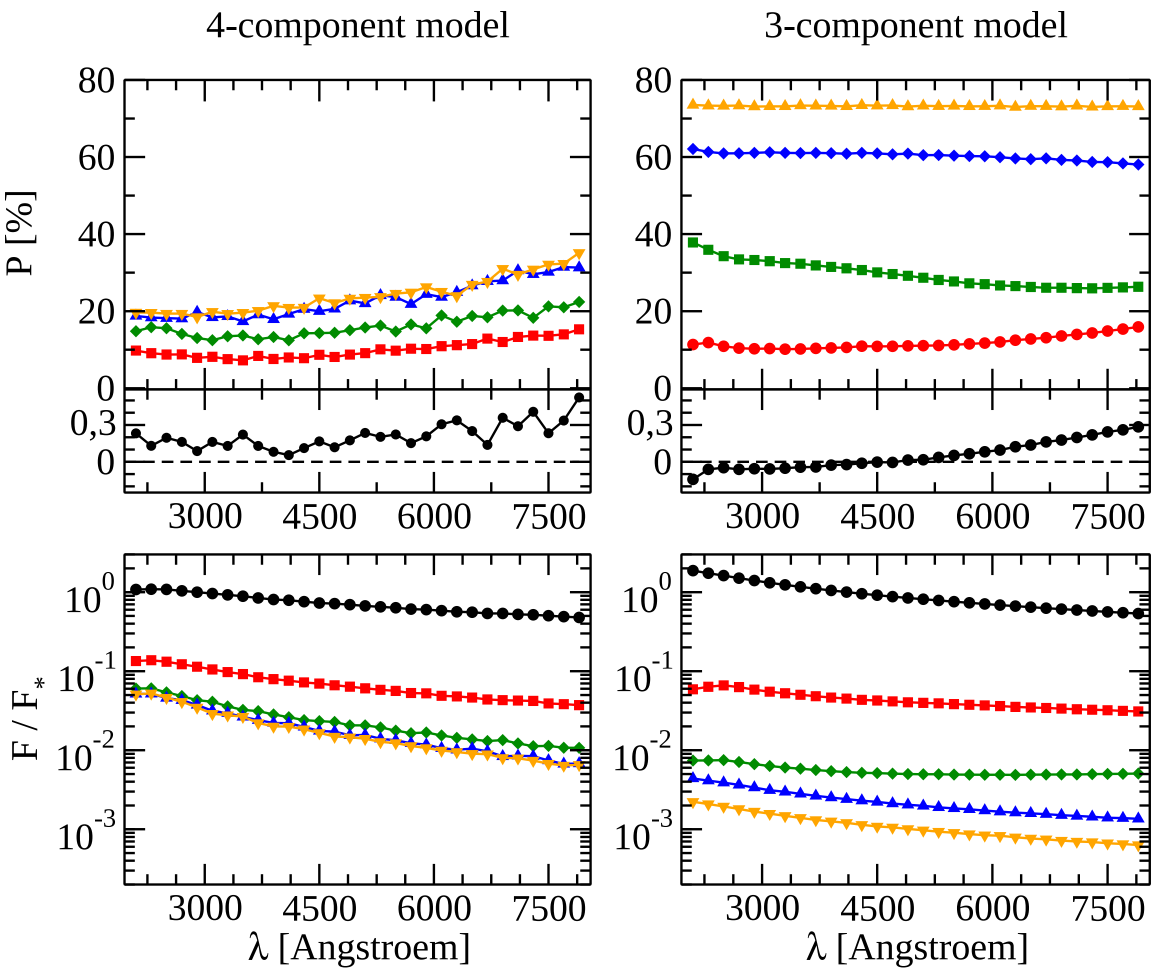

Fig. 1. Modeling the unified scheme of a thermal AGN. **Left column**: the 4-component model as described in the text. **Right column**: the 3-component model lacking the NLR region as presented in Marin et al. (2012b). Both figures show the polarization percentage, P, as a function of viewing inclination i measured from the torus axis and the fraction, F/F_*, of the central flux, F_*; Legend: $i = 84°$ (orange triangles with points to the bottom), $i = 73°$ (blue triangles with points to the top), $i = 60°$ (green diamonds), $i = 46°$ (red squares), $i = 26°$ (black circles).

3-component model. Additional depolarization occurs because the photons passing through the NLR have to undergo more scattering events before they escape from the model region. Due to the wavelength-dependence of Mie scattering, the presence of the NLR also has an effect on the spectral shape of P.

Compared to the observed optical/UV polarization of Seyfert-2 galaxies (Kay 1994, $P_{\rm obs} \leq 10\%$), our theoretical polarization is still too high, even though the presence of the NLR helps to approach the observed range of P. As discussed in Marin et al. (2012b), our model so far assumes a uniform density in all reprocessing regions. However, there are observational hints that the torus and the polar outflows should be fragmented (Nenkova et al. 2008, 2010). Preliminary modeling of such a clumpy reprocessing structure with *STOKES* indicates that the resulting polarization further decreases with respect to a uniform density model and may allow us to explain the observations of Kay (1994). Apart from the polarization, the bottom of Fig. 1 shows that the total (polarized + non-polarized) spectrum F/F_* decreases towards longer wavelengths in both models. This is another signature of the wavelength-dependent Mie scattering cross section and phase function. Also, a faint scattering feature at 2175 Å due to the carbonacious dust component is visible. When the NLR is included, the additional polar dust scattering increases the total flux scattered towards edge-on inclinations.

For type-1 objects our modeling shows that the additional dust scattering in the NLR can switch the $\vec{E}$-vector from a parallel to a perpendicular polarization state. While for the 3-component model the polar view exhibits parallel polarization below 4500 Å (Fig.1, top right, lower panel), the polarization is perpendicular across the whole wavelength range in the 4-component case (Fig.1, top left, lower panel). Given the resulting weak percentage ($< 0.5\%$) of the perpendicular polarization, this model setup is coherent with the so-called *polar scattering dominated* AGN (Smith et al. 2002). Such type-1 AGN present a perpendicular, optical polarization rising towards the blue that Smith et al. (2002) explained by dust extinction along a line of sight passing through the upper layers of the torus material. Our model qualitatively produces a similar wavelength-dependent polarization, but at a much lower viewing angle. However, the relatively low optical depth of the polar dust scattering does not reproduce the full extend of the observed rise in P towards the blue end of the spectrum.

4 Summary and conclusions

To study the impact of the NLR on the polarization spectra in the optical/UV, we presented results for a 4-component reprocessing model computed with *STOKES*. In comparison with the 3-component model presented in Marin et al. (2012b), where polar dust scattering was absent, it appeared that the NLR cloud globally decreases the amount of polarization at type-2 viewing angles and may enforce perpendicular polarization also at type-1 viewing angles. The spectral shape of the polarization changes due to the additional Mie scattering in the polar directions.

An important conclusion to draw from this initial investigation is that the production of parallel polarization at type-1 viewing angles may become more difficult when the NLR is taken into account. It remains to investigate in a forthcoming study, to which extend the scattering origin of parallel polarization in type-1 AGN can be maintained. Inclusion of clumpy reprocessing media is important in such an investigation. On the positive side, the NLR helps to explain the observed degree of continuum polarization in type-2 objects.

The NLR region is an important ingredient of the unified AGN scheme, and if the extended outflows in Seyfert-2 galaxies are indeed photo-ionization by the emission of an obscured primary source, then the NLR is expected to sustain the same half-opening angle as the obscuring circumnuclear matter (Bianchi et al. 2012). Constraints on the half-opening angle of the NLR could thus provide estimates of the relative ratio of Seyfert-1 to Seyfert-2 galaxies in the local universe. The geometrical shape of the NLR region may also help us to determine if the symmetry implied by the unified model is broken (see Raban et al. 2009; Goosmann & Matt 2011; Marin et al. 2012a, for a study on NGC 1068). Such an asymmetry may explain the high degree of parallel polarization detected in peculiar objects like Mrk 231 (Gallagher et al. 2005) and ultimately lead to a better understanding of the launching of outflows inside the funnel of the circumnuclear medium.

This research was supported by the French *GdR* PCHE and the research grant ANR-11-JS56-013-01.

References

Antonucci, R. 1993, ARA&A, 31, 473
Antonucci, R. R. J. 1982, Nature, 299, 605
Antonucci, R. R. J. 1983, Nature, 303, 158
Antonucci, R. R. J. 1984, ApJ, 281, 112
Bianchi, S., Maiolino, R., & Risaliti, G. 2012, Advances in Astronomy, 2012
Capetti, A., Axon, D. J., Macchetto, F. D., Marconi, A., & Winge, C. 1999, Mem. Soc. Astron. Italiana, 70, 41
Cracco, V., Ciroi, S., di Mille, F., et al. 2011, MNRAS, 418, 2630
Gallagher, S. C., Schmidt, G. D., Smith, P. S., et al. 2005, ApJ, 633, 71
Goosmann, R. W. & Gaskell, C. M. 2007, A&A, 465, 129
Goosmann, R. W. & Matt, G. 2011, MNRAS, 415, 3119
Hoenig, S. F., Kishimoto, M., Antonucci, R., et al. 2012, ArXiv e-prints
Kay, L. E. 1994, ApJ, 430, 196
Marin, F., Goosmann, R., & Dovčiak, M. 2012a, Journal of Physics Conference Series, 372, 012065
Marin, F. & Goosmann, R. W. 2011, in SF2A-2011: Proceedings of the Annual meeting of the French Society of Astronomy and Astrophysics, ed. G. Alecian, K. Belkacem, R. Samadi, & D. Valls-Gabaud, 597–600
Marin, F., Goosmann, R. W., Gaskell, C. M., Porquet, D., & Dovciak, M. 2012b, ArXiv e-prints (1209.2915)
Mathis, J. S., Rumpl, W., & Nordsieck, K. H. 1977, ApJ, 217, 425
Nenkova, M., Sirocky, M. M., Nikutta, R., Ivezić, Ž., & Elitzur, M. 2008, ApJ, 685, 160
Nenkova, M., Sirocky, M. M., Nikutta, R., Ivezić, Ž., & Elitzur, M. 2010, ApJ, 723, 1827
Raban, D., Jaffe, W., Röttgering, H., Meisenheimer, K., & Tristram, K. R. W. 2009, MNRAS, 394, 1325
Smith, J. E., Young, S., Robinson, A., et al. 2002, MNRAS, 335, 773
Wilson, A. S. & Ulvestad, J. S. 1983, ApJ, 275, 8